Full Paper

Reactive Molecular Dynamics Study on the Effect of H$_2$O on the Thermal Decomposition of Ammonium Dinitramide

Tao Zeng,[a, b] Rongjie Yang,[a, b] Dinghua Li,[a] Jianmin Li,[a, b] Xiaoyan Guo,*[a] and Peng Luo[c]

Abstract: Ammonium dinitramide (ADN) is a halogen-free green oxidizer, which is widely used in energetic materials because of its positive oxygen balance and low characteristic signal. However, ADN is easy to absorb moisture, which affects its storage and safety performances. It is of great significance to study the effect of water on its thermal decomposition mechanism. In this paper, the thermal decomposition processes of the ADN with water contents of 0%, 1%, 2%, 5%, and 10% are simulated by large-scale reactive molecular dynamics simulations. The reaction pathway and the evolution of the main products are analyzed in detail. The results show that the ADN is not stable and decompose easily, namely ADN→NH$_3$(NH$_4$) + HN$_3$O$_4$(N$_3$O$_4$). The H$_2$O has a significant effect on the thermal decomposition of the ADN. The water contents of 2% and 5% can better promote the decomposition of the ADN and the degree of decomposition is also more thorough.

1 Introduction

The ammonium dinitramide (ADN), as a new generation of the high energy oxidizer, is considered to be a preferable alternative to the traditional ammonium perchlorate (AP) oxidizer because of the advantage of positive oxygen balance and low characteristic combustion signal [1–9]. Therefore, ADN has attracted a great deal of interests in the energetic materials community. The thermal decomposition mechanism of ADN has been explored experimentally and theoretically. Kazakov et al. [10] investigated the kinetics of the thermal decomposition of ADN in sulfuric acid, nitric acid, and anhydrous acetic acid solutions and proposed the likely mechanism of the decomposition of dinitramide. Andreev et al. [11] studied the kinetics of the main products of thermal decomposition of ADN in the melt. They found the isotope composition of nitrogen-containing gases evolved by the decomposition of ^{15}NH$_4$N(NO$_2$)$_2$ and NH4^{15}N(NO$_2$)$_2$. Löbbecke et al. [12] studied the thermal properties and decomposition behavior of ADN. The results showed that the pathway of the main decomposition was that ADN →NH$_4$NO$_3$ + N$_2$O and NH$_4$NO$_3$→N$_2$O + H$_2$O. Tompa [13] determined the kinetic constants of decomposition for ADN and prilled ADN with differential scanning calorimetry (DSC) and thermogravimetric analysis (TG). Brill et al. [14] described the rapid pyrolysis chemistry of films of ADN using the T-jump/Fourier transform inrared spectroscopy, indicating that ADN was highly exothermic very early in the process of the ADN decomposition. Rossi et al. [15] studied the response of ADN to thermal stress under low heating rate conditions. They found that ADN decomposed into HN(NO$_2$)$_2$ and NH$_3$. Velardez et al. [16] calculated the melting point and some liquid properties of ADN with molecular dynamics simulation at the different pressures and temperatures. The normal melting temperature of the ideal crystal calculated was in the range 474~476 K. Zhu et al. [17] studied the mechanism for sublimation of NH$_4$N(NO$_2$)$_2$ using generalized gradient approximation plane-wave density functional theory. The results showed that water molecules can increase the sublimation enthalpy of ADN. Alavi et al. [18] investigated the proton transfer in gaseous (ADN) clusters up to (ADN)$_2$ with density-functional theory. The results showed that proton transfer in the ADN monomer did not occur between the hydrogen dinitramide and ammonia units. Wang et al. [5] determined the vibrational frequencies of the reactants, the products, the geometries, and the transition states involved in intramolecular hydrogen-transfer and decomposition reactions of the free gas-phase using CBS-QB3 method. They found that the intramolecular hydrogen-transfer reaction of ADN was more feasible than that of HN$_3$O$_4$.

The energy release of the energetic materials, such as ADN, which is very explosive, is a dangerous and complex

[a] T. Zeng, R. Yang, D. Li, J. Li, X. Guo
School of Materials Science and Engineering, Beijing Institute of Technology, Beijing, China, 100081
*e-mail: gxy@bit.edu.cn

[b] T. Zeng, R. Yang, J. Li
State key Laboratory of Explosion Science and Technology, Beijing Institute of Technology, Beijing, China, 100081

[c] P. Luo
Xi'an North Hui An Chemical Industries Co. Ltd, Xi'an, China, 710032

(a) The 2×2×3 supercell

(b) Monomolecular structure of ADN
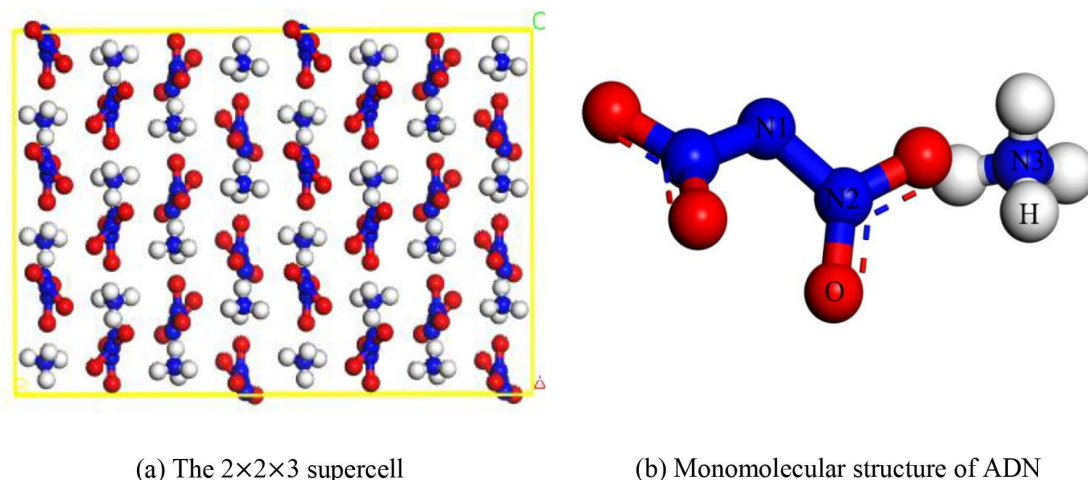
Figure 1. The 2×2×3 supercell model of the ADN.

(a) Water content of 1%

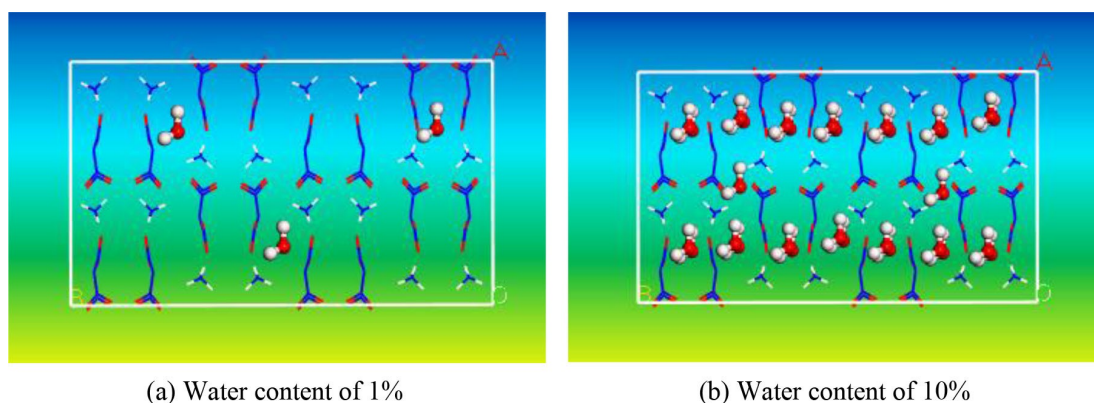(b) Water content of 10%

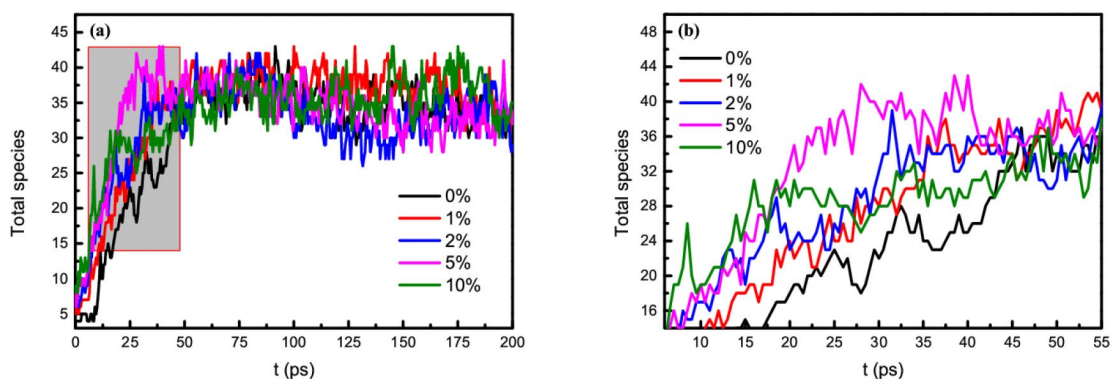**Figure 2.** The models of the ADN with water contents of 1% and 10%.

Figure 3. Evolution of total species of ADN for the different water content systems.

chemical reaction process. It is difficult to investigate the thermal decomposition mechanism experimentally. Reactive molecular dynamics (RMD) simulations with ReaxFF force field developed by van Duin [19] can describe the detailed process of chemical reactions at atomic level and femtosecond scale. In view of the shortcomings of the ReaxFF force field underestimating the long-range van der Waals (vdW) interaction, the correction term based on the low-gradient model was introduced to correct the dispersion effect of the ReaxFF force field. Through this mod-
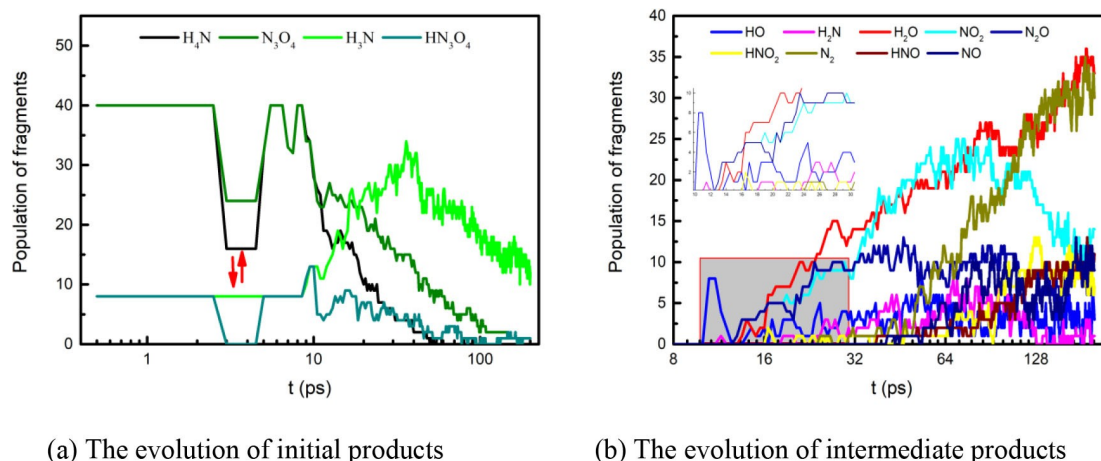
(a) The evolution of initial products

(b) The evolution of intermediate products

Figure 4. The evolution of the main products with time for the dry ADN.

(a) Water content of 1%

(b) Water content of 2%

(c) Water content of 5%
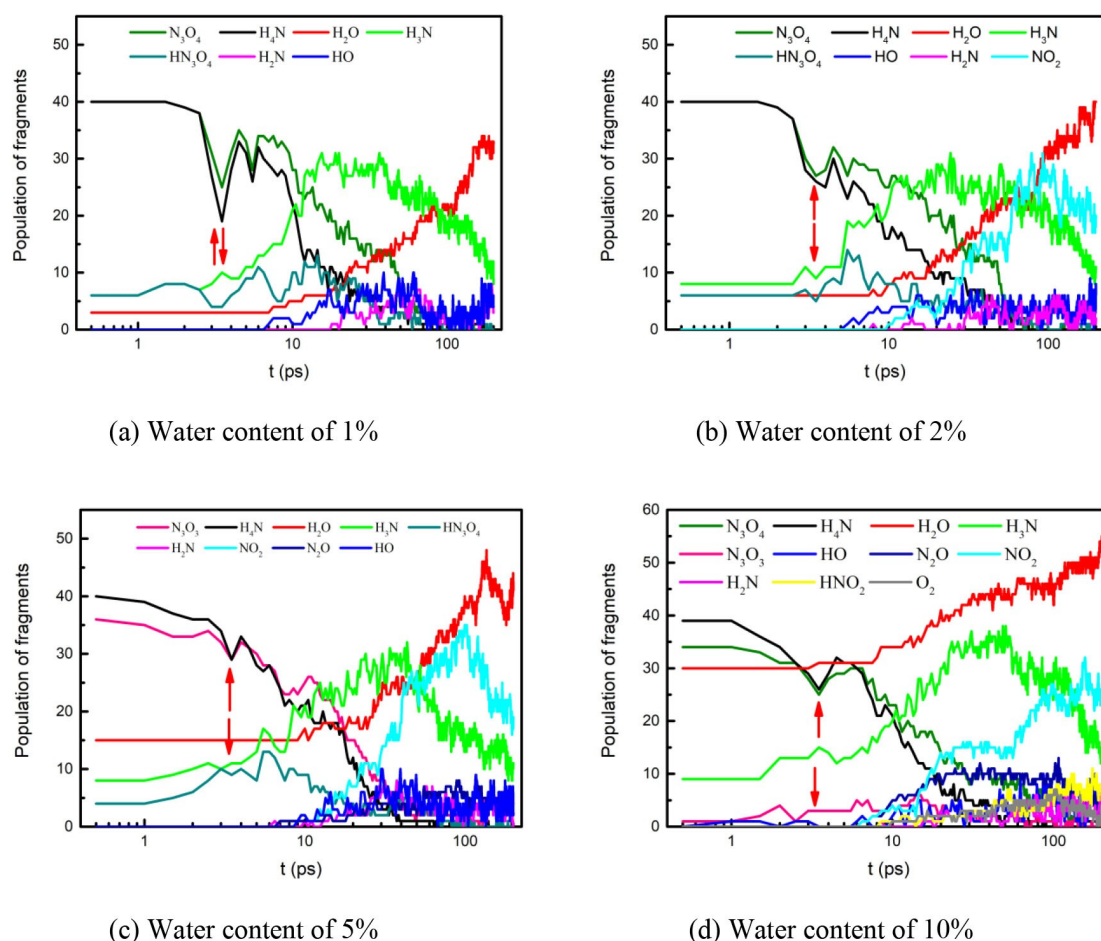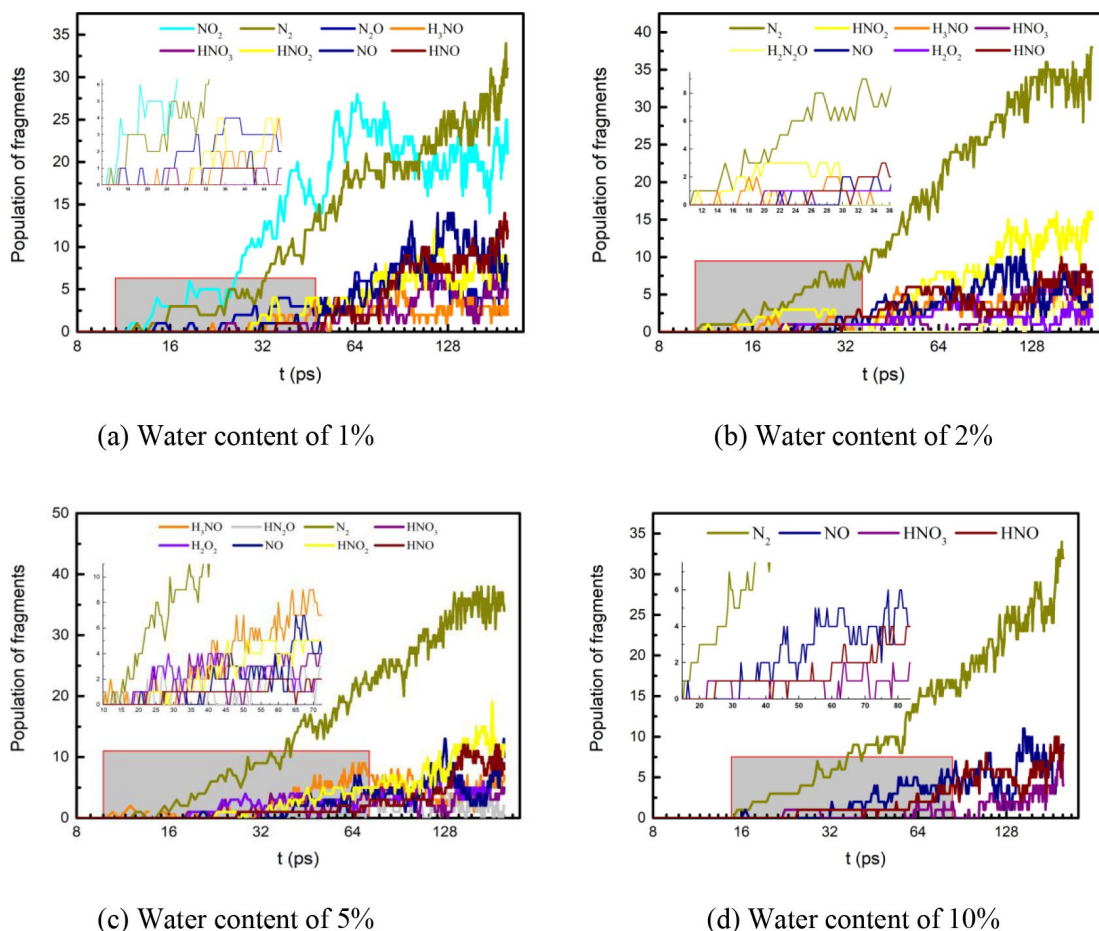

(d) Water content of 10%

Figure 5. Evolution of main initial products for the different water contents with time.

ification, the reaction force field developed based on the first-principle (DFT) can reasonably describe the long-range interaction. The ReaxFF-lg force field can accurately predict the lattice parameters, sublimation enthalpy, and state function of molecular crystals of energetic materials [20]. The RMD method with ReaxFF-lg force field, which is comparable in accuracy to quantum mechanics and is fast enough to handle millions of atoms, has been widely em-

(a) Water content of 1%

(b) Water content of 2%

(c) Water content of 5%

(d) Water content of 10%

Figure 6. Evolution of main intermediate products in the different water contents with time.

(a) Main decomposition reaction pathway

(b) Snapshot at 150 ps for water content of 5%.
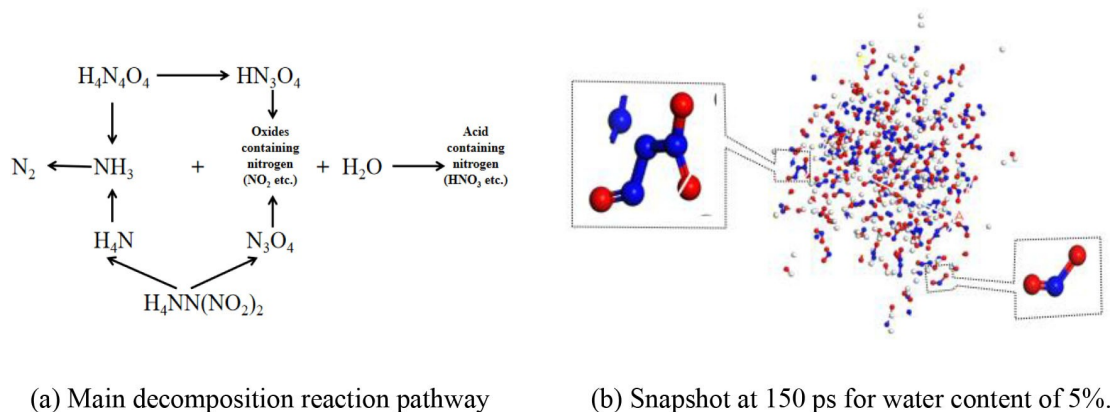
Figure 7. The thermal decomposition pathway of ADN with water.

ployed to explore the thermal decomposition reaction mechanism of many energetic materials, such as HMX [21], TATP [22], NM [23, 24], TNT [25], RDX [26], HNS [27] and CL-20 [28].

In spite that many researches have been performed on the thermal decomposition of the ADN, the few studies on the effect of the H₂O on the ADN thermal decomposition have been reported. In addition, ADN is easy to absorb moisture, which affected its performance seriously, so it is of great significance to explore the influence of the H₂O on its thermal decomposition mechanism. In this paper, we analyze the reaction mechanism, the reaction pathway, and
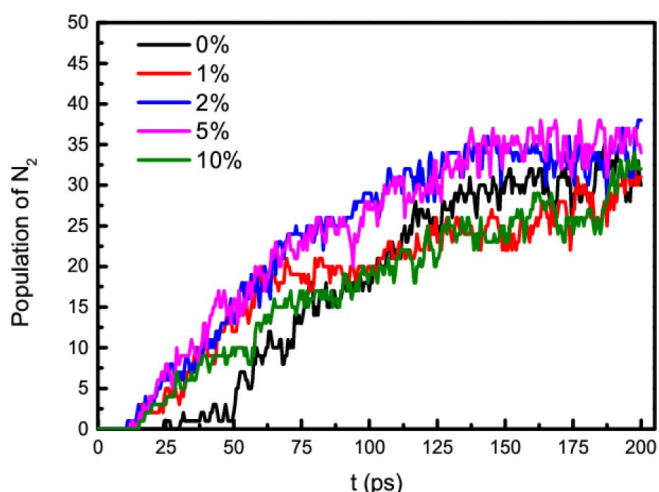
Figure 8. Evolution of main product N_2 with time for the five different water contents.

the main products of thermal decomposition for the ADN with the water contents of 0%, 1%, 2%, 5%, and 10%.

2 Computational Methods

2.1 Molecular Modeling and Simulation Details

(1) Molecular modeling

We perform the simulations using the LAMMPS Molecular Dynamics Simulator with the ReaxFF-lg force field. The unit cell of the ADN is created according to the literature [29]. And a 2×2×3 supercell including 48 ADN molecules is constructed, as is shown in Figure 1. On the basis of the supercell, the water molecules of 0, 3, 6, 15 and 30 are added in the Z direction, and the molecular models of the ADN with the water content of 1% (containing 3 water molecules) and 10% (containing 30 water molecules) are shown in Figure 2 (H, O, and N atoms are colored white, red, and blue, respectively).

(2) The selection of NVT ensemble (canonical ensemble)

The relaxation of the initial cell is carried out at room temperature (298 K). At room temperature, the level of water content has little impact on the pressure of the whole system; second, ADN is a kind of high-energy material. During the decomposition of ADN, it is very easy to have violent and rapid chemical reactions at high temperature (3000 K). In this process, it is generally believed that the volume of the system has not changed. Using NVT ensemble (that refers to the constant number of atoms, constant volume, and constant temperature, respectively) can better describe and reflect the decomposition law of ADN in the actual application process, which is more instructive to the use of

ADN; last, the density has a signification effect on the decomposition of energetic materials [30,31]. Based on the above reasons, the NVT ensemble is applied.

(3) Simulation details

Firstly, the five crystal supercells with the water contents of 0%, 1%, 2%, 5%, and 10% are relaxed and optimized for 20 ps with the NVT ensemble (the canonical ensemble). The temperature is controlled at room temperature (298 K) with Berendsen thermostat. Secondly, the five optimized systems are used as the initial structure for five subsequent separate molecular dynamics (MD) simulations. They are heated from 298 to 3000 K, respectively. NVT-MD simulations are then carried out for 200 ps to ensure that the reaction reaches equilibrium. The temperature is controlled with the Berendsen thermostat with damping constant of 100.0 fs [27]. The time step is 0.01 fs. A 0.3 bond order cutoff for all atom pairs is applied to identify the molecular species. In order to avoid the confusion of the real bond breaking and formation due to the instantaneous fluctuation in the bond order, we define the time window for counting the new bond formation and breaking process as 0.5 ps. The dynamic trajectories, connection table of the atoms, and molecular species obtained by the reactive molecular dynamics are determined every 500 steps. These data are used to analyze the decomposition process of ADN and its hydrate, including the evolution of the main products and the reaction pathway.

2.2 Fragment Analysis

The trajectory of complex reactions that occur during ReaxFF simulations are analyzed using a self-written perl script. The script reads in the LAMMPS output trajectory file and then calculates the chemical bonds and specifies the molecules for each frame structure. In each frame, each molecule is output as a mol (filename extension) format file, and InChI (The International Union of Pure and Applied Chemistry (IUPAC) gives the unique identification code for the chemical structure of each compound) [32] analysis is performed using Open Babel (The Open Source Chemistry Toolbox) [33] to determine the unique identification of the molecule. According to InChI markers, the species, structure, and number of molecules are counted and output.

3 Results and Discussion

3.1 Parameters Verification of ReaxFF MD Applicability to ADN

The decomposition mechanism of energetic materials, such as HMX [21], TATP [22], NM [23,24], TNT [25], RDX [26], HNS [27] and CL-20 [28], have been studied under different con-

ditions using ReaxFF MD. To verify the portability of ReaxFF MD for ADN oxidizer, the lattice parameters, the density, and the bond lengths of atom pairs (The particular positions of N1, N2, N3, O, and H are marked in Figure 1) are calculated with ReaxFF MD. For the pure ADN unit cell structure, a $2\times2\times3$ supercell structure is constructed. In the supercell structure, 48 molecules are included. Firstly, the atomic position in the supercell is optimized to obtain the structure with the minimum energy. Then, the isothermal-isothermal (NPT) MD simulation is carried out to relax the internal stresses and obtain the initial structure (volume V_0) for zero pressure and $T_0 = 298$ K temperature [21,27,28]. The Berendsen thermostat and the Berendsen barostat are used for temperature and pressure. After 10 ps of NPT-MD simulation, the equilibrium ADN crystal structure is obtained. The results of the calculation are shown in Table 1, which are almost consistent with the results obtained by the density functional theory (DFT) [34] and the experiment [35].

In addition, the accuracy of ReaxFF in describing the dissociation behavior of a gas-phase ADN molecule is examined. The dissociation barriers along several channels are calculated utilizing the nudged elastic band (NEB) technique with ReaxFF. Two possible initial steps in the pyrolysis route are considered according to previous studies by breaking the following bonds: (1) N−NH₃; (2) N−NO₂. So, two possible dissociation paths are calculated. The results are compared to those bond dissociation energies obtained by ab initio calculations of DFT with the generalized gradient approximation (GGA) (Table 2). The calculation shows that dissociation barriers are qualitatively and quantitatively predicted by the potential obtained from ReaxFF. The dissociation of the N−NH₃ bond is most favored, whereas the dissociation of the N−NO₂ bonds are least energetically favorable, which is consistent with the experimental results [4]. We compared the N−NO₂ dissociation barrier of ADN with RDX [36] (174.1 kJ/mol), HMX [36] (179.2 kJ/mol), TNAZ [36] (183.8 kJ/mol), Tetryl [36] (120.1 kJ/mol), and CL-20 [37] (171.5, 158.2, and 145.0 kJ/mol), indicating that thermal sensibility of ADN is relatively more stable.

These show that ReaxFF MD has good accuracy for ADN, and the decomposition process of ADN and its hydrate can be analyzed by ReaxFF MD.

Table 2. Dissociation Barriers (in kJ/mol) of a Gas-Phase ADN Molecule.

Reaction channel	Breaking bond	ReaxFF	DFT [17]
ADN→HN₃O₄+NH₃	N-NH₃	200.7	181.2
ADN→H₃N₃O₂+NO₂	N-NO₂	247.2	244.0

3.2 Evolution of Total Species for the Different Water Contents

Evolution of total species of ADN thermal decomposition with time for the different water contents is shown in Figure 3. From Figure 3(a), the total species of the five systems first increase rapidly, then decrease slightly, and finally tend to be stable, indicating that the decomposition reactions eventually reach equilibrium after experiencing the violent reactions. Figure 3(b) is the local enlargement. It is found that the amount of total species for the ADN with water are much larger than that for the dry ADN (the water content of 0%) between 0 to 40 ps. Surprisingly, the amount of the ADN with water content of 2% and 5% are initially lower than that of 10% but eventually exceeded it. The results show that the water content of 2% and 5% can better accelerate the decay of ADN than the other three.

3.3 Evolution of Main Products for Different Water Contents

To analyze the evolution of products of the ADN thermal decomposition for the different water contents, a series of Matlab scripts are written to process the output and trajectory file calculated by LAMMPS. We divide the products into two kinds: the initial products first appearing before 10 ps (including 10 ps) and the intermediate products first appearing after 10 ps. Furthermore, a fragment is defined as a main product when its maximum frequency of appearance is above 5 during the whole thermal decomposition with a lifetime of ≥20 ps. In the calculation time of 200 ps, we define the duration of species from generation (first appearance) to disappearance as the lifetime of species. Because the decomposition reaction is from complete molecules to small molecules (fragments), it is the process of breaking old bonds and generating new bonds. Moreover, if only one chemical bond breaks in the system, it is difficult to be reflected in species information and elementary reactions. In this paper, a method is proposed to analyze the initial chemical reaction from the perspective of chemical

Table 1. Lattice parameters, the density, and bond lengths of ADN.

crystal	method	a (Å)	b (Å)	c (Å)	ρ (g·cm⁻³)	N2-O	N1-N2
ADN	DFT	6.98	12.12	5.41	1.82 [29]	1.24	1.36
	ReaxFF-lg	6.91	11.79	5.61	1.83	1.31	1.49

bond formation and breakage. By tracking the connection of small molecules (or fragments) at different times, and counting the small molecules (or fragments) whose connection changes in a very short time, the formation and breakage of different types of chemical bonds are obtained.

In order to obtain the initial reaction path of thermal decomposition of the reactants, according to the analysis method of Wen et al. [38], the chemical bond connection between atoms at different times was analyzed. Select the molecule whose atomic connection changes at the adjacent moments, then get the elementary reaction equation, and count the times of this type of elementary reaction within this time interval (that is, the frequency of this reaction). The main products, their lifetime, and the frequencies of their appearance during the whole process of thermal decomposition as well as their apparent reaction equation (Molecular formulas consist of fragments) when they first appear in the different water contents are obtained (as shown in Table 3). The products in the Table 3 are arranged in chronological order based on when first appear.

From Table 3, the common main products of the ADN thermal decomposition in the different water contents are H_3N, H_2O, N_2, NO_2, H_2N, NO, HNO_2, HO, and HNO. In addition, we also find slight differences in the main products obtained for the five different water contents. For the ADN with water contents of 2% and 5%, H_2O_2 is formed, whereas O_2 is formed only for that of 10% (see Table 3), indicating that the water content in the ADN has a significant effect on the thermal decomposition path. Therefore, the main initial products and intermediate products are analyzed, respectively.

3.4 The Evolution of the Main Initial Products

The evolution of the main products with time for the dry ADN are given in Figure 4. From Table 3 and Figure 4, ADN is initially broken down into $NH_3(NH_4)$ and $HN_3O_4(N_3O_4)$ in a very short time, indicating that the ADN is not stable and decompose easily, namely $ADN \rightarrow NH_3(NH_4) + HN_3O_4(N_3O_4)$.

In Figure 4(b), the NO_2 and N_2O also begin to appear when the HO begins to appear after HN_3O_4, indicating that $HN_3O_4 \rightarrow HO + N_3O_3$ and $N_3O_3(N_3O_4) \rightarrow NO_2 + N_2O$. (The snapshots of N_3O_3 and NO_2 are shown in the Figure 7(b)). The numbers of $NH_3(NH_2)$ and $NO_2(N_2O)$ first increase, then decrease while the N_2 begins to appear, indicating that $NH_3(NH_2) + NO_2(N_2O) \rightarrow N_2$.

The evolution of the main initial products for the ADN with water contents of 1%, 2%, 5%, and 10% are given in Figure 5. Compared with Figure 4, it is found that H_2O has a significant effect on $HN_3O_4(N_3O_4)$ and NH_4. Furthermore, the different water contents have different effects on the $HN_3O_4(N_3O_4)$ and NH_4. The obvious differences are marked by the red arrow in the Figure 4(a) and 5. The addition of H_2O can reduce the initial amounts of $HN_3O_4(N_3O_4)$ in the system. Instead, the amounts of N_3O_3, NO_2, N_2O, and HO in

the thermal decomposition of the ADN with water begin to increase earlier than that of the dry ADN. We take NO_2 as an example. While the NO_2 for the dry ADN first appears at 12.95 ps, the NO_2 for the ADN with water contents of 1%, 2%, 5%, and 10% first appear at 11.95, 9.65, 6.95 and 5.05 ps, respectively (see Table 3). This shows that H_2O promotes the decomposition of $HN_3O_4(N_3O_4)$.

3.5 The Evolution of the Main Intermediate Products

The evolution of the main intermediate products for the ADN with water contents of 1%, 2%, 5%, and 10% are given in Figure 6. Combined with Figure 5, it is found that the total species of the main products increase, and the more the total species of the main initial products, the less that of the main intermediate products of the ADN for the different water contents. This indicates that H_2O can accelerate the decay of the intermediate products during the process of the ADN thermal decomposition. In addition, it is noted that the O_2 can be generated in the ADN with the water content of 10%, and the H_2O_2 can be generated in the ADN with water contents of 2% and 5%. It can be inferred that $NH_3(NH_2) + NO_2(N_2O) \rightarrow H_2O_2 + N_2$ and $H_2O_2(H_2O) \rightarrow O_2$. The main reaction pathway could be identified, as is shown in the Figure 7.

3.6 Evolution of Main Product N_2 for the five Different Water Contents

Evolution of the main product N_2 for the ADN with the five different water contents are shown in Figure 8. At 40 ps, the growth rate of N_2 for the ADN with water content of 10% begins to slow down while the growth rate of N_2 for the ADN with water content of 1% begins to decrease at 60 ps. Their amounts of N_2 are exceeded by that for the dry ADN at 105 ps. The product N_2 initially increases and then trends to be stable with time. The growth rates and amounts of N_2 with time for the ADN with water contents of 2% and 5% are similar, which are higher than the other three. The results show that the water contents of 2% and 5% can better promote the decay of the ADN, and its degree of decomposition is more thorough, which are almost consistent with the literature[39–42]. This may be because when the dry ADN combines with H_2O, water can induce protons to transfer from NH_4^+ to $N(NO_2)_2^-$, forming $H_3N \ldots HON(O)NNO_2 \cdot nH_2O$ complex and the formation of this complex requires more energy, resulting in an increase in the sublimation enthalpy of ADN. This can explain the abnormal decomposition phenomenon that the decomposition rate decreases when the water content is 1%, but increases when the water content is 2% and 5%. When the water content is 10%, water can inhibit the chemical reaction $HN(NO_2)_2 + H_2O \rightarrow H_3O^+ + N(NO_2)_2^-$, preventing the conversion of nitrogen oxides to the corresponding acid, which inhibits

Reactive Molecular Dynamics Study on the Effect of H₂O on the Thermal Decomposition of Ammonium Dinitramide

Table 3. The main products with high frequencies and reaction time.

Water content	Products	Reaction time/ps	Highest frequencies	Reaction equation
0%	H_3N	0~200	35	$H_4N_7O_8 = H_3N + HN_6O_8$
	HN_3O4	0~200	15	$HN_6O_8 = N_3O_4 + HN_3O_4$
	HO	10.1~200	9	$HN_3O_4 = HO + N_3O_3$
	H_2N	11.2~200	8	$HO + 2H_4N = H_2 + H_2N + H_5NO$
	H_2O	12.8~200	36	$H_5NO = H_3N + H_2O$
	NO_2	12.95~200	27	$N_3O_3 = NO_2 + N_2O$
	N_2O	12.95~200	13	$N_3O_3 = NO_2 + N_2O$
	HNO_2	16.05~200	13	$HN_3O_4 = HNO_2 + N_2O_2$
	N_2	24.15~200	35	$H_3N_3O = H_3NO + N_2$
	HNO	37.9~200	13	$H_3N_4O_4 = H_2N_3O_3 + HNO$
	NO	40.75~200	13	$N_3O_2 = N_2O + NO$
1%	H_2O	0~200	34	$H_5NO = H_2O + H_3N$
	H_3N	0~200	31	$H_4N_7O_8 = H_3N + HN_6O_8$
	HN_3O_4	0~193.45	13	$HN_6O_8 = N_3O_4 + HN_3O_4$
	H_2N	5.75~200	9	$H_4N_4O_4 = N_3O_4 + H_2N + H_2$
	HO	7~200	11	$HN_3O_4 = HO + N_3O_3$
	NO_2	11.95~200	28	$HN_3O_3 = NO_2 + HN_2O$
	N_2	12.05~200	34	$HN_2O = HO + N_2$
	N_2O	14.5~200	11	$N_3O_3 = NO_2 + N_2O$
	H_3NO	21.6~200	7	$H_3N_6O_8 + H_5N_3O_3 = HO + H_2N_6O_7 + H_3NO + H_2N_2O_2$
	HNO_3	24.4~200	8	$HN_3O_3 + H + N_5O_4 = HN_3O_4 + 2\,N_2 + HNO_3$
	HNO_2	29.4~200	12	$H_4N_2O_2 = H_3N + HNO_2$
	NO	31.4~200	16	$N_3O_4 = N_2O_3 + NO$
	HNO	34.3~200	14	$H_2NO + H_3N_2O = HNO + H_4N_2O$
2%	H_2O	0~200	41	$H_4NO = H_2O + H_2N$
	H_3N	0~200	31	$H_4N_7O_8 = H_3N + HN_6O_8$
	HN_3O_4	0~200	14	$N_6O_8 + HN_6O_8 = 3\,N_3O_4 + HN_3O_4$
	HO	5.1~200	10	$H_3N_3O_4 = HO + H_2N_3O_3$
	H_2N	7.7~200	7	$H_4NO = H_2O + H_2N$
	NO_2	9.65~200	31	$N_3O_3 = N_2O + NO_2$
	N_2	11~200	38	$N_3O_2 = NO_2 + N_2$
	HNO_2	11.45~200	17	$H_2N_3O_3 = HN_2O + HNO_2$
	H_3NO	13.85~200	8	$H_5NO_2 = H_2O + H_3NO$
	HNO_3	19.85~200	8	$HN_3O_3 = N_2 + HNO_3$
	H_2N_2O	20.05~200	7	$H_2O + N_2 + N_3O_5 = NO_2 + N_2O_3 + H_2N_2O$
	NO	21.9~200	12	$HN_3O_2 = HN_2O + NO$
	H_2O_2	22.5~200	5	$O + HN_2O + H_2O + NO = HN_3O_2 + H_2O_2$
	HNO	25.1~200	10	$H_3N_4O_3 + H_6N_7O_6 = H_6N_5O_3 + HNO + H_2N_5O_5$
5%	H_2O	0~200	48	$H_2N_3O_5 = N_3O_4 + H_2O$
	H_3N	0~200	33	$H_4N_7O_8 = H_3N + HN_6O_8$
	HN_3O_4	0~196.95	14	$H_2N_6O_8 = 2HN_3O_4$
	H_2N	6.51~99.35	8	$H_3N + N_3O_4 = HN_3O_4 + H_2N$
	NO_2	6.95~200	35	$N_3O_3 = NO_2 + N_2O$
	N_2O	6.95~200	8	$N_3O_3 = NO_2 + N_2O$
	HO	7.15~200	11	$H_6NO_2 = H_5NO + HO$
	H_3NO	10.5~200	9	$H_8N_2O_2 = H_4N + HO + H_3NO$
	HN_2O	12.15~200	6	$HN_3O_3 = NO_2 + HN_2O$
	N_2	12.35~200	39	$N_3O_4 + HN_3O_4 + N_3O_2 = HN_6O_8 + NO_2 + N_2$
	HNO_3	13.85~200	6	$HN_4O_6 = N_3O_3 + HNO_3$
	H_2O_2	18.3~200	10	$H_2N_3O_4 + H_5NO_2 = H_3N + NO_2 + H_2N_2O_2 + H_2O_2$
	NO	20.5~200	13	$N_6O_6 = N_5O_5 + NO$
	HNO_2	22.8~200	19	$H_5N_4O_5 + H_4N_2O_2 = 2H_3N + HN_3O4 + HO + HNO_2$
	HNO	26.7~200	12	$H_5NO_4 = HNO + H_4O_3$
10%	H_2O	0~200	55	$H_2N_3O_5 = N_3O_4 + H_2O$
	H_3N	0~200	40	$H_4N_7O_8 = H_3N + HN_6O_8$
	N_3O_3	0~200	7	$H_2N_6O_8 = H_2N_3O_5 + N_3O_3$
	HO	0.95~200	11	$H_4NO = H_3N + HO$
	N_2O	5.05~200	13	$N_3O_3 = N_2O + NO_2$
	NO_2	5.05~200	32	$N_3O_3 = N_2O + NO_2$

Table 3. continued

Water content	Products	Reaction time/ps	Highest frequencies	Reaction equation
	H_2N	8.15~200	8	$H_4N = H_2 + H_2N$
	HNO_2	8.25~200	11	$H_2N_3O_4 = HNO_2 + HN_2O_2$
	O_2	9.1~200	7	$H_5N_4O_5 = O_2 + H_5N_4O_3$
	N_2	15.45~200	34	$H_4N_3O = H_4NO + N_2$
	NO	16.45~200	11	$HN_3O_2 = HN_2O + NO$
	HNO_3	22.2~200	8	$H_2N_4O_7 = HN_3O_4 + HNO_3$
	HNO	24.9~200	11	$H_6N_5O_5 = H_5N_4O_4 + HNO$

the decay of ADN. These show that the amount of water content also has a great influence on the formation of N_2 during the process of the ADN thermal decomposition.

4 Conclusion

The thermal decomposition processes of the ADN with water contents of 0%, 1%, 2%, 5%, and 10% are calculated by large-scale reactive molecular dynamics simulations. ADN is initially broken down into $NH_3(NH_4)$ and $HN_3O_4(N_3O_4)$ in a very short time, indicating that the ADN is not stable and decompose easily, namely $ADN \rightarrow NH_3 + HN_3O_4$. The H_2O has a significant effect on the products HN_3O_4 (N_3O_4) and can accelerate their decay during the process of the thermal decomposition, leading to accelerating decay of the ADN. Compared with the water content of 0%, 1%, and 10%, the water contents of 2% and 5% can better promote the decay of the ADN and the degree of decomposition is also more thorough. The amount of water content has a great influence on the thermal decomposition of the ADN. In addition, it is inferred that NH_3 (NH_2) + NO_2 (N_2O) $\rightarrow H_2O_2 + N_2$ and H_2O_2 (H_2O) $\rightarrow O_2$.

References

[1] S. Borman, Advanced Energetic Materials Emerge for Military and Space Applications, *Chem. Eng. News.* **1994**, *72(3)*, 18–22.

[2] J. C. Bottaro, P. E. Penwell, R. J. Schmitt, 1,1,3,3-Tetraoxo-1,2,3-Triazapropene Anion, a New Oxy Anion of Nitrogen: the Dinitramide Anion and Its Salts, *J. Am. Chem. Soc.* **1997**, *119*, 9405–9410.

[3] G. Santhosh, S. Venkatachalam, K. N. Ninan, R. Sadhana, S. Alwan, V. Abarna, M. A. Joseph, Adsorption of Ammonium Dinitramide (ADN) from Aqueous Solutions. 1. Adsorption on Powdered Activated Charcoal, *J. Hazard. Mater.* **2003**, *98*, 117–126.

[4] R. Yang, P. Thakre, V. Yang, Thermal Decomposition and Combustion of Ammonium Dinitramide (Review), *Combustion, Explosion and Shock Waves* **2005**, *41*, 657–679.

[5] Z. Wang, T.-L. Zhang, M.-J. Li, Q. Xu, R. Wang, S. Roy, X. Yu, L. Jin, Computational Study of the Decomposition Mechanisms of Ammonium Dinitramide in the Gas Phase, *Mol. Phys.* **2018**, *116*, 1756–1771.

[6] O. A. Luk'yanov, V. P. Gorelik, and V. A. Tartakovskii, Dinitramide and its Salts. 1. Synthesis of Dinitramide Salts by De-cyanoethlation Reaction of N, N-Dinitro-b-aminopropionitrile, *Russ. Chem. Bull.* **1994**, *43*, 89–92.

[7] O. A. Luk'yanov, Yu. V. Kopnova, T. A. Klimova, and V. A. Tartakovskii, Dinitramide and its Salts. 2. Dinitramide in Michael- and retro- Michael-type reactions, *Russ. Chem. Bull.* **1944**, *43*, 1200–1202.

[8] O. A. Luk'yanov, O. V. Anikin, V. P. Gorelik, and V. A. Tartakovsky, Dinitramide and its Salts. 3. Metallic salts of dinitramide, *Russ. Chem. Bull.* **1994**, *43*, 1457–1461.

[9] V. A. Shlyapochnikov, N. O. Cherskaya, O. A. Luk'yanov, V. P. Gorelik, V. A. Tartakovsky, Dinitramide and its salts. 4. Molecular structure of dinitramide, *Russ. Chem. Bull.* **1994**, *43*, 1522–1525.

[10] A. I. Kazakov, Y. I. Rubtsov, G. B. Manelis, Kinetics and Mechanism of Thermal Decomposition of Dinitramide, *Propell. Explos. Pyrot.* **1999**, *24*, 37–42.

[11] A. B. Andreev, O. V. Anikin, A. P. Ivanov, V. K. Krylov, Z. P. Pak, Stabilization of Ammonium Dinitramide in the Liquid Phase, *Russ. Chem. Bull.* **2000**, *49*, 1974–1976.

[12] S. Löbbecke, T. Keicher, H. Krause, A. Pfeil, The New Energetic Material Ammonium Dinitramide and Its Thermal Decomposition, *Solid State Ionics.* **1997**, *101–103*, 945–951.

[13] A. S. Tompa, Thermal Analysis of Ammonium Dinitramide (ADN). *Thermochim. Acta.* **2000**, *357–358*, 177–193.

[14] T. B. Brill, P. J. Brush, D. G. Patil, Thermal Decomposition of Energetic Materials 58. Chemistry of Ammonium Nitrate and Ammonium Dinitramide Near the Burning Surface Temperature, *Combust. Flame.* **1993**, *92*, 178–186.

[15] M. J. Rossi, J. C. Bottaro, D. F. McMillen, The Thermal Decomposition of the New Energetic Material Ammoniumdinitramide ($NH_4N(NO_2)_2$) in Relation to Nitramide (NH_2NO_2) and NH_4NO_3, *Int. J. Chem. Kinet.* **1993**, *25*, 549–570.

[16] G. F. Velardez, S. Alavi, D. L. Thompson, Molecular Dynamics Studies of Melting and Liquid Properties of Ammonium Dinitramide, *J. Chem. Phys.* **2003**, *119*, 6698–6708.

[17] R. S. Zhu, H. L. Chen, M. C. Lin, Mechanism and Kinetics for Ammonium Dinitramide (ADN) Sublimation: A First-Principles Study, *J. Phys. Chem. A.* **2012**, *116*, 10836–10841.

[18] S. Alavi, D. L. Thompson, Proton Transfer in Gas-Phase Ammonium Dinitramide Clusters, *J. Chem. Phys.* **2003**, *118*, 2599–2605.

[19] A. C. T. van Duin, S. Dasgupta, F. Lorant, W. A. Goddard, ReaxFF: A Reactive Force Field for Hydrocarbon, *J. Phys. Chem. A.* **2001**, *105*, 9396–9409.

[20] L. Liu, C. Bai, H. Sun, W. A. Goddard, Mechanism and Kinetics for the Initial Steps of Pyrolysis and Combustion of 1,6-Dicyclopropane-2,4-Hexyne from ReaxFF Reactive Dynamics, *J. Phys. Chem. A.* **2011**, *115*, 4941–4950.

[21] L. Zhang, S. V. Zybin, A. C. T. van Duin, S. Dasgupta, W. A. Goddard, E. M. Kober, Carbon Cluster Formation During Thermal

Decomposition of Octahydro-1,3,5,7-Tetranitro-1,3,5,7-Tetrazo-cine and 1,3,5-Triamino-2,4,6- Trinitrobenzene High Explosives from ReaxFF Reactive Molecular Dynamics Simulations, *J. Phys. Chem. A.* **2009**, *113*, 10619.

[22] A. C. T. van Duin, Y. Zeiri, F. Dubnikova, R. Kosloff, W. A. Goddard, Atomistic-Scale Simulations of the Initial Chemical Events in the Thermal Initiation of Triacetonetriperoxide, *J. Am. Chem. Soc.* **2005**, *127*, 11053–11062.

[23] F. Guo, X. L. Cheng, H. Zhang, Reactive Molecular Dynamics Simulation of Solid Nitromethane Impact on (010) Surfaces Induced and Nonimpact Thermal Decomposition, *J. Phys. Chem. A.* **2012**, *116*, 3514–3520.

[24] S. P. Han, A. C. T. van Duin, W. A. Goddard, A. Strachan, Thermal Decomposition of Condensed-Phase Nitromethane from Molecular Dynamics from Reaxff Reactive Dynamics, *J. Phys. Chem. B.* **2011**, *115*, 6534–6540.

[25] D. Furman, R. Kosloff, F. Dubnikova, S. V. Zybin, W. A. Goddard, N. Rom, B. Hirshberg, Y. Zeiri, Decomposition of Condensed Phase Energetic Materials: Interplay Between Uni- and Bimolecular Mechanisms, *J. Am. Chem. Soc.* **2014**, *136*, 4192–4200.

[26] A. Strachan, E. M. Kober, A. C. T. van Duin, J. Oxgaard, W. A. Goddard, Thermal Decomposition of RDX from Reactive Molecular Dynamics, *J. Chem. Phys.* **2005**, *122*, 54502.

[27] L. Chen, H. Wang, F. Wang, D. Geng, J. Wu, J. Lu, Thermal Decomposition Mechanism of 2,2′,4,4′,6,6′-Hexanitrostilbene by ReaxFF Reactive Molecular Dynamics Simulations. *J. Phys. Chem. C.* **2018**, *122, 19309–18*.

[28] F. P. Wang, L. Chen, D. Geng, J. Wu, J. Lu, C. Wang, Thermal Decomposition Mechanism of CL-20 at Different Temperatures by ReaxFF Reactive Molecular Dynamics Simulations, *J. Phys. Chem. A.* **2018**, *122*, 3971–3979.

[29] R. Gilardi, J. Flippen-Anderson, C. George, R. J. Butcher, A New Class of Flexible Energetic Salts: The Crystal Structures of the Ammonium, Lithium, Potassium, and Cesium Salts of Dinitramide, *J. Am. Chem. Soc.* **1997**, *119*, 9411–9416.

[30] N. Rom, S. V. Zybin, A. C. T. V. Duin, W. A. Goddard, Y. Zeiri, G. Katz, Density-Dependent Liquid Nitromethane Decomposition: Molecular Dynamics Simulations Based on ReaxFF, *J. Phys. Chem. A.* **2011**, *115*, 10181–10202.

[31] F. P. Wang, L. Chen, D. S. Geng, J. Y. Lu, J. Y. Wu, Effect of Density on Thermal Decomposition Mechanism of ε-CL-20: A Re-axFF Reactive Molecular Dynamics Simulation Study, *Phys. Chem. Chem. Phys.* **2018**, *10*, 1039.C8CP03010 C-.

[32] S. Heller, A. McNaught, S. Stein, D. Tchekhovskoi, I. Pletnev, InChI-the Worldwide Chemical Structure Identifier Standard, *Journal of Cheminformatics.* **2013**, *5*, 7.

[33] N. M. O'Boyle, M. Banck, C. A. James, C. Morley, T. Vandermeersch, G. R. Hutchison, Open Babel: An Open Chemical Toolbox, *Journal of Cheminformatics.* **2011**, *3*, 33.

[34] W. Zhu, T. Wei, W. Zhu, H. Xiao, Comparative DFT Study of Crystalline Ammonium Perchlorate and Ammonium Dinitramide, *J. Phys. Chem. A.* **2008**, *112*, 4688–4693.

[35] A. Hahma, H. Edvinsson, H. Östmark, The Properties of Ammonium Dinitramine (ADN): Part 2: Melt Casting, *Journal of Energetic Materials.* **2010**, *28*, 114–138.

[36] C. J. Wu, L. E. Fried, *First-principles Study of High Explosive Decomposition Energetics*, Office of Scientific & Technical Information Technical Reports, **1998**.

[37] F. P. Wang, *Molecular Dynamics study on Chemical Reaction Mechanism of CL-20 under Heat and Shock*, Beijing **2019**. P. 18. (in Chinese).

[38] Y. S. Wen, X. G. Xue, X. P. Long, C. Y. Zhang, Cluster Evolution at Early Stages of 1,3,5-Triamino-2,4,6-trinitrobenzene under Various Heating Conditions: A Molecular Reactive Force Field Study, *J. Phys. Chem. A* **2016**, *120*, 22, 3929–3937.

[39] I. B. Mishra, T. P. Russell, Thermal Stability of Ammonium Dinitramide, *Thermochim. Acta.* **2002**, *384*, 47–56.

[40] A. N. Pavlov, V. N. Grebennikov, L. D. Nazina, G. M. Nazin, G. B. Manelis, Thermal Decomposition of Ammonium Dinitramide and Mechanism of Anomalous Decay of Dinitramide Salts, *Russ. Chem. Bull.* **1999**, *48*, 50–54.

[41] S. B. Babkin, A. N. Pavlov, G. M. Nazin, Anomalous Decomposition of Dinitramide Metal Salts in the Solid Phase, *Russ. Chem. Bull.* **1997**, *46*, 1844–1847.

[42] A. I. Kazakov, Y. I. Rubtsov, G. B. Manelis, L. P. Andrienko, Kinetics of the Thermal Decomposition of Dinitramide, *Russ. Chem. Bull.* **1998**, *47*, 39–45.